Ultrahigh Electrical Conductivity of Graphene Embedded in Metals

Mu Cao, Ding-BangXiong Li Yang, Shuaishuai Li, Yiqun Xie, Qiang Guo, Zhiqiang Li, Horst Adams, Jiajun Gu, Tongxiang Fan, Xiaohui Zhang, and Di Zhang**

There is a need for ultra-conductors because they can lead to higher efficiency and less energy consumption in a wide range of applications. However, the improvement of the electrical conductivity of conventional conductors is limited by the purity of the metal and the ability to grow single crystal structures. Here, by embedding graphene in metals (Cu, Al, and Ag), the trade-off between carrier mobility and carrier density is overcome in a graphene layer through a specific interface design and morphology control, enabling high electron mobility and high electron density simultaneously. As a result, a maximum electrical conductivity three orders of magnitude higher than the highest on record (more than 3,000 times higher than that of Cu) is obtained in such embedded graphene. By using graphene as reinforcement, an electrical conductivity as high as ~117% of the International Annealed Copper Standard and significantly higher than that of Ag is achieved in bulk graphene/Cu composites with an extremely low graphene volume fraction of only 0.008%. The results are of significance when enhancing efficiency and saving energy in electrical and electronic applications of metals, and are also beneficial for fundamental research on electron behavior in graphene.

1. Introduction

Extensive research efforts have been dedicated to improving electrical conductivity of Cu, such as producing Cu with a purity as high as 7N or with an oxygen content as low as 1 x 10^{-4} %. However, an improvement of only ~3% has been achieved for highly refined Cu compared to the electrical conductivity officially recorded already about 100 years ago. A higher electrical conductivity of 106-109% of the International Annealed Copper Standard (IACS) can be obtained in a Cu single crystal. However, the improvements obtained by reducing electron scattering centers (such as heteroatoms and grain boundaries) in both metal purification and single crystal growth control have been pushed to their physical limits and inevitably lead to increased cost. Moreover, metals with high purity and less grain boundaries usually have insufficient mechanical strength for many practical applications.

Producing metal-based composites by incorporating non-metal reinforcements with excellent electrical conductivity is a promising strategy for enhancing the electrical conductivity. In theory, aligned single-walled carbon nanotubes (SW-CNT) were expected to enhance the electrical conductivity of Cu by 100% with a volume fraction of 30-40%.[1] However, the practical challenge lies in the sufficient purification of metallic SW-CNTs and the actual making of such composite materials.[2] Graphene, a single layer of sp^2-bonded carbon atoms, has been extensively studied as a cornucopia of electrical transport phenomena.[3-16] Because of its remarkable intrinsic carrier mobility [17] and unique carrier transport properties,[12-16] graphene is expected to be an excellent conductor. However, its maximum electrical conductivity still needs to be determined, and realizing such superior electrical properties in macroscopic composite materials is a great challenge.

The electrical conductivity of a material depends on both the mobility and the density of charge carriers. In graphene, ultrahigh carrier mobilities are achieved at a relatively low electron density. For instance, a carrier mobility value exceeding

M. Cao, Prof. D.-B. Xiong, Prof. Q. Guo, Prof. Z. Li, Prof. J. Gu, Prof. T. Fan, Prof. D. Zhang State Key Laboratory of Metal Matrix Composites Shanghai Jiao Tong University Shanghai 200240, China
E-mail: xiongdingbang@sjtu.edu.cn; zhangdi@sjtu.edu.cn

Prof. L. Yang
Department of Physics
Washington University in St. Louis
One Brookings Drive, St. Louis, MO 63130, USA

S. S. Li, Prof. Y. Xie
Department of Physics
Shanghai Normal University
100 Guilin Road, Shanghai 200234, China

Prof. H. Adams
Adamco Inc
2223 Watts Street, Houston, TX 77030, USA

Dr. X. Zhang
CRRC Industrial Institute Co., Ltd. Beijing
100067, China

The ORCID identification number(s) for the author(s) of this article can be found under https://doi.org/10.1002/adfm.201806792
DOI: 10.1002/adfm.201806792

2 x 10^5 cm^2 V^{-1} s^{-1} was measured at a carrier density of ~2 x 10^{11} cm^{-2} in a suspended, single-layer graphene sample.[18] A much higher mobility value in excess of 10^7 cm^2 V^{-1} s^{-1} has been realized in a graphene layer on a graphite substrate with an ultralow carrier density (n ~ 3 x 10^9 cm^{-2}).[19] This trade-off causes the electrical conductivity of graphene to be comparable to that of a bulk metal with a low electron mobility but very high electron density. Moreover, the high electron mobility in graphene strongly depends on its structural integrity and the type of substrate. Approaches to ensure a high carrier mobility in graphene include lowering the defect density,[18,20,21] suspending graphene,[13,22] depositing graphene onto high-quality substrates,[23,24] and covering graphene with high-k dielectrics.[25,26] However, these rather sophisticated methods make it difficult to transfer any superior carrier transport properties on the molecular-level to a macroscopic bulk material. Not surprisingly, the electrical conductivity of most reported graphene (or graphene derivative)-reinforced metal matrix composites does not surpass that of the pure metal matrices.[27-30] In this work, we demonstrate that graphene sheets deposited by chemical vapor deposition (CVD) and embedded inside metal matrices (Cu, Ag, and Al) can provide local, ultrahigh electrical conductivity inside the composite material. That conductivity can be up to three orders of magnitude higher than that of most conductive pure metals at room temperature, showing a remarkable potential for enhancing the electrical performance of metals.

2. Results and Discussion

The sample preparation method used is described in Figure S1 in the Supporting Information. In a first step, a graphene monolayer is deposited on both sides of a commercial Cu foil **(Figure 1a)** via a CVD process. Then graphene/copper (Gr/Cu) composites (Figure 1c) are produced by stacking and hot pressing *i* layers of the Gr/Cu/Gr foils **(Figure 1b)**. Using this fabrication method, large bulk composite samples can be made, their thickness being directly proportional to the number of foils used. The CVD process on Cu foils can provide high-quality graphene films [31] yielding coatings with homogeneous and defect free graphene mono-layers. Aligning the individual graphene layers in the resulting laminated structure allows to take advantage of the anisotropic properties of the 2D material. The weak adhesion energy of monolayer graphene grown on copper [32] can be improved by using a hot-pressing process,[28] leading to a strong mechanical bond at the Cu/Gr/Cu interface **(Figure 1d, g)**. In an ideal composite, all graphene layers embedded inside the Cu matrix would be bilayers because the composite is produced by stacking monolayer-Gr/Cu/monolayer-Gr foils. However, in a real sample, some trilayer or tetralayer graphene layers are also present. This is caused by unavoidable inhomogeneities in the CVD coating process (Figure S2, Supporting Information).

To evaluate the electrical conductivity of individual graphene layers embedded inside a macroscopic Gr/Cu laminated composite, a tunneling atomic force microscope (PF-AFM, Dimension FastScan Bio, Bruker) **(Figure 2a)** was used to map the electrical conductivity in a defined area[33,34] across the Cu/Gr/Cu interface at room temperature (Figures S3-S5, Supporting Information). A typical current mapping image **(Figure 2b)** shows that the electrical current drastically increases along the graphene layer. In some areas, the current is more than 3000 times higher than that measured in the surrounding Cu matrix. The peak amplitude fluctuations in the electrical current are attributed to inhomogeneities in the graphene layers, as seen in the transmission electron microscope (TEM) image **(Figure 1g)**. For reference, the same measurement was also carried out with a control sample created from stacked and hot-pressed pristine Cu foils not containing any graphene. In this case, no increment or fluctuation in the electrical current was observed in the entire analyzed area (Figure S6, Supporting Information).

We were able to transfer part of the ultrahigh electrical conductivity detected at nanoscale to macroscopic bulk

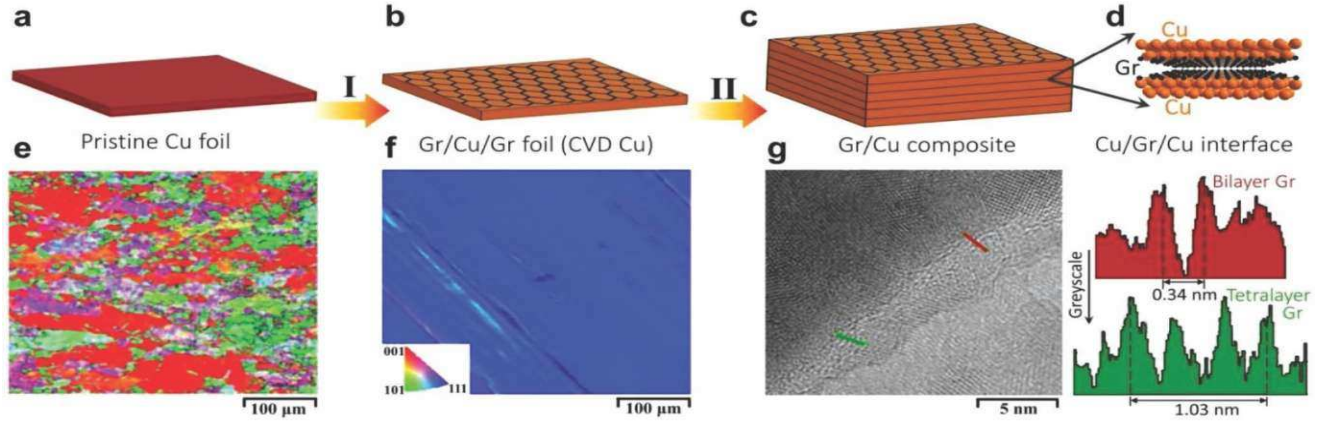

Figure 1. Fabrication of Gr/Cu composites with aligned CVD graphene. a-c) Stacking method for multilayered composites: I) Depositing graphene on both sides of pristine polycrystalline Cu foil via a CVD process; II) stacking *i* layers of Gr/Cu/Gr foils and hot pressing at 50 MPa and 900 °C. d) Schematic of the Cu/Gr-layers/Cu interface structure. e,f) EBSD images of the Cu foils before and after graphene deposition. g) TEM image of the Cu/Gr/Cu interface, showing mostly bilayer graphene as well as some trilayer or tetralayer graphene, as indicated by the grayscale section analyses of the two high-intensity peaks (red) and four high-intensity peaks (blue) separated by an expected interplanar spacing of 0.34 nm.

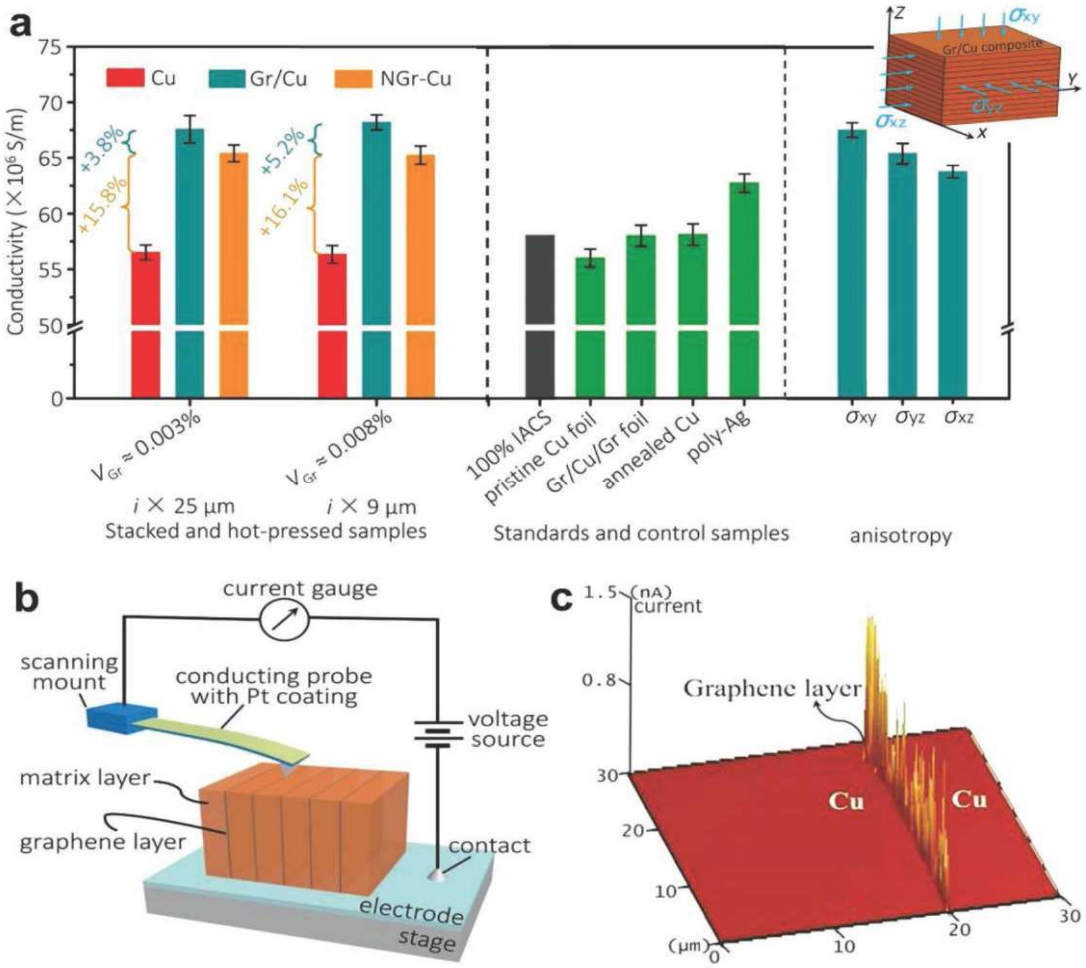

Figure 2. Macroscale and nanoscale electrical conductivity measurements. a) The contributions to the electrical conductivity increase were analyzed for two Gr/Cu multilayered composites with Cu layer thicknesses of 9 and 25 µm respectively. The Cu and NGr-Cu specimens were fabricated by stacking and hot pressing the corresponding coated Cu foils and the naked Cu foils from which the grown-on graphene was removed by reactive oxygen-ion etching. V_{Gr} was calculated using 0.7 nm as the thickness of bilayer graphene. For comparison, the electrical conductivities of IACS standard samples and select other reference samples are shown in the middle column. All samples (100% IACS, pristine copper foil, Gr/Cu/Gr foil, polycrystalline Ag (poly-Ag), and annealed Cu) were fabricated by stacking, hot pressing, and annealing (where applicable) them under the same temperature conditions as used in the CVD process. The right column shows the electrical conductivities measured at the different sides of a bulk Gr/Cu laminated composite sample using a standard four-probe setup, revealing an anisotropic electrical conductivity. The error bars in all the histograms represent the standard variation of the averaged electrical conductivity of samples from different batches, but not for an individual measurement. b) Schematic of a PF-AFM nanoscale current mapping setup used for analyzing the Gr/Cu multilayered composites. c) Current mapping image of a 30 µm x 30 µm Cu/Gr/Cu interface area. The peak current along the graphene layer is three orders of magnitude higher than that measured in the surrounding pure Cu matrix.

samples at room temperature. The electrical conductivities of bulk Gr/Cu composite samples were evaluated using a standard four-probe method (Figure S7, Supporting information). The results show that the electrical conductivity depends on the volume fraction of graphene (V_{Gr}) in the bulk Gr/Cu composite. The V_{Gr} in the Gr/Cu composite can be changed by varying the thickness of the stacked Cu foils. We analyzed four different commercially available copper foils with thicknesses of 9, 25, 37, and 45 µm (Figure S8, Supporting information). Considering that each of the bilayer graphene layers has a thickness of h ~ 0.7 nm, the V_{Gr} is estimated to be in the range of <0.002% to ~0.008% for the four different Gr/Cu composites. The electrical conductivity increases as the thickness of the Cu layers decreases and V_{Gr} increases (Figure S9, Supporting information). However, the effect is relatively small because the volume fraction of graphene is only in the ppm range for all four composites. Additionally, an anisotropy of the electrical conductivity was observed in the laminated Gr/Cu bulk composites **(Figure 2c)**. The highest electrical conductivity occurs along the in-plane direction (σ^{xy}), while a much lower conductivity was measured perpendicular to the Gr/Cu interface(σ^{xz}). This effect is directly related to the true 2D nature of graphene.

The V_{Gr}-dependency and anisotropic conductivity behavior provide clear evidence that indeed the graphene layers are the reason for the enhanced electrical conductivity of the Gr/Cu composites. Of all the investigated Gr/Cu composites, the highest measured electrical conductivity was

σ_{xy} = 68.2 x 10^6 S m^{-1} for the Gr/Cu composite with the thinnest Cu layers (i.e. 9 µm), which also corresponded to the highest volume fraction of graphene, V_{Gr} = 0.008% **(Figure 2c)**. Expressed in IACS (58.1 x 10^6 S m^{-1}), this value is equivalent to an electrical conductivity of ~117.4% IACS, which is substantially higher than that of the best metal conductor, i.e. silver (~108% IACS at room temperature). Even the electrical conductivity of Gr/Cu composites with a Cu layer thickness of 25 µm (V_{Gr} ~0.003%) was determined to be only slightly lower, i.e. 116.3% IACS, which is still much better than the conductivity of silver.

The macroscopic enhancement of the electrical conductivity in a Gr/Cu bulk composites can be attributed to a combination of two factors: i) the electrical properties of graphene and ii) microstructural changes of the Cu matrix. The latter can be quantified by measuring the electrical conductivity of bulk samples without graphene (NGr-Cu), which were fabricated by removing the graphene from the Gr/Cu/Gr foil using reactive oxygen-ion etching, and subsequent stacking and hot pressing the resulting naked CVD Cu substrate foils. The direct contribution of graphene to the total conductivity can be determined by subtracting the electrical conductivity of the sample without graphene (NGr-Cu) from the conductivity of an otherwise identical sample with graphene (Gr/Cu). Two different Gr/Cu composite sample sets with Cu layer thicknesses of 9 and 25 µm respectively were analyzed. As seen in **Figure 2c**, the contribution from the microstructural changes of the Cu matrix dominates the macroscale electrical conductivity enhancement in the Gr/Cu composites. By subtracting the contribution from the microstructural changes of the Cu matrix, the direct contribution of graphene to the overall conductivity is 3.8% and 5.2% in the Gr/Cu composites with Cu layer thicknesses of 25 and 9 µm, respectively. Although the net contribution from graphene is not high, the efficiency of the electrical conductivity enhancement is truly remarkable considering the volume fraction of graphene being only V_{Gr} = 0.003% and 0.008% in the respective Gr/Cu composites. The electrical conductivity of the Gr/Cu composite is expected to be further increased by 2-3 orders of magnitude by fabricating Gr/Cu sub-micro-/nano-laminated composites, i.e. decreasing the thickness of Cu foils and thus increasing the volume fraction of graphene.[35-39] The enhancement efficiency is three orders of magnitude higher than that presented in any previous report.[40] Based on our macroscale measurements, the electrical conductivities inside the embedded graphene layers are 650 and 1267 times higher than that of the pure Cu matrix for V_{Gr} = 0.003% and 0.008%, respectively. These results are in the same order of magnitude as the values that were obtained using the nanoscale PF-AFM method.

As seen in the electron backscattering diffraction (EBSD) image in **Figure 1**, the pristine Cu foil used for CVD is polycrystalline without any obvious texture **(Figure 1e)**. However, after the CVD process, a strong Cu(111) orientation is detected, accompanied by a significant grain coarsening **(Figure 1f)**. To evaluate the influence of the Cu matrix texture and its microstructure on the electrical conductivity of the embedded graphene, three Cu/Gr/Cu sandwiched samples with different phase relations/orientations between graphene and copper were fabricated and analyzed **(Figure 3).** Individual substrates of polycrystalline Cu (poly-Cu) **(Figure 3a)**, Cu(111) **(Figure 3b)**, and Cu(100) **(Figure 3c)** single crystals were used. For the Cu(111) and Cu(100) single-crystal samples, monolayer graphene was directly deposited on their surfaces using the above described CVD process, while for the polycrystalline Cu sample, a free standing monolayer of graphene was peeled off from a previously CVD-coated foil and transferred onto the surface of the polycrystalline Cu to prevent any microstructural change of the copper. Layered samples were obtained by stacking and hot pressing the corresponding Gr/Cu slices to form Cu/Gr/Cu sandwiched samples.

A comparison of the current flow data of the three different samples obtained by using the PF-AFM mapping method described above reveals that all three samples have current peaks along the graphene layers, but the average current amplitudes follow the sequence Cu(111)/Gr/Cu(111) > Cu(100)/ Gr/Cu(100) > poly-Cu/Gr/poly-Cu **(Figure 3)**. These results are consistent with the degree of lattice matching between the Gr layer and Cu matrix. Cu(111)/Gr/Cu(111) has the best lattice

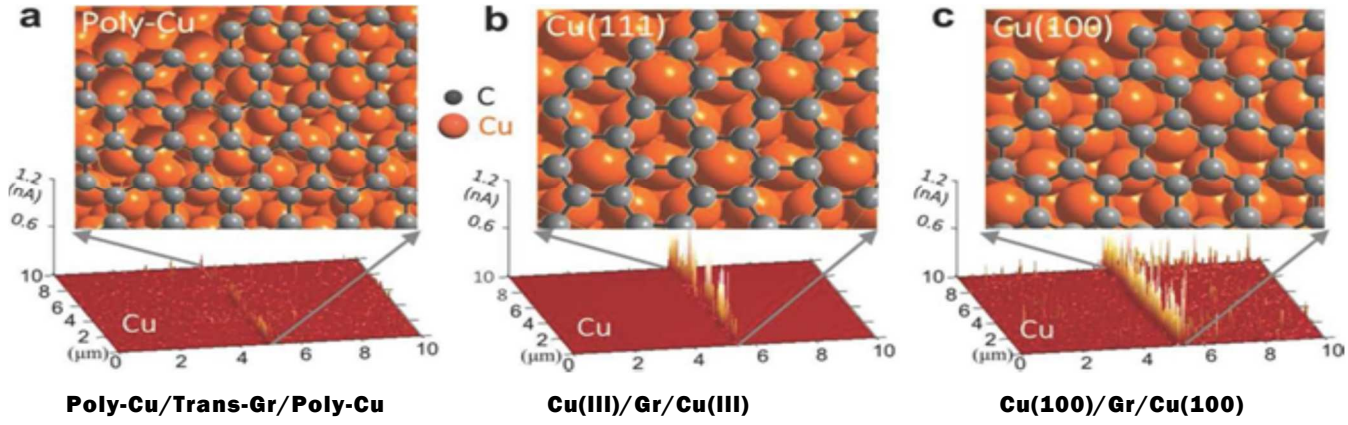

Figure 3. A comparison of current flow along the interface area in Gr/Cu composites with different matrices of a) polycrystalline Cu, b) Cu(111) single crystal, and c) Cu(100) single crystal. The crystallographic schematics show various phase relations between the Gr layers and Cu matrices. Trans-Gr means that the graphene was peeled off of a Gr/Cu/Gr foil and transferred onto a target substrate.

matching because of the same threefold symmetry and a very similar lattice constant between graphene (2.46 Å) and Cu(111) (2.56 Å).[41,42] However, the graphene transferred onto the poly-crystalline Cu has unavoidable defects and disruptions, such as wrinkles, ripples, and folds. These defects might also have adversely affected the graphene current transport properties in the poly-Cu/Gr/poly-Cu sample. [43]

The intrinsic properties of graphene depend on its quality and morphology, such as its defect density, layer number, and lateral size. In the following part of this work, we investigate the influence of the number (n) of graphene layers embedded inside a copper matrix on the electrical conductivity. By carefully controlling the carbon source concentration (gas flow) and growth time during the CVD process, graphene with well-defined layer numbers ranging from n = 1 to n~10 was deposited on both sides of Cu substrate foils. The structural integrity and homogeneity of the deposited graphene were determined by obtaining Raman spectra **(Figure 4a,b)** after the deposition process. Following the fabrication scheme depicted in **Figure 1**, five Gr/Cu multi- layered composites (II to VI in **Figure 4c**) were obtained. The total number of Gr layers was twice the number of the Gr inlays due the stacking process. Composite I, with monolayer graphene inlays, was fabricated by alternately stacking monolayer-Gr/Cu/monolayer-Gr foil and the naked CVD Cu foil (the grown graphene was removed from the Gr/Cu/Gr foil by reactive oxygen-ion etching). A comparison of the current mapping data of the different Gr/Cu composites shows that the electrical conductivity in the graphene layers decreases with increasing layer numbers. In the Gr/Cu composites with a layer number n > 6–10 (3–5 layers × 2 in composite IV), while the electrical peak current is remarkably attenuated. According to the first-principles calculation results based on the density functional theory for a practical model of a Cu/bilayer-Gr/Cu interface **(Figure 5a,b)**, we postulate that the high electrical conductivity of embedded graphene is due to a doping effect that leads to an increased carrier density and very high carrier mobility in graphene. We found that a primitive cell of bilayer graphene (containing four carbon atoms) obtains an average of ~0.24 electrons (Table S1, Supporting information) from neighboring Cu atoms in the matrix, indicating a doping effect in the graphene with an estimated electron density of ~4.3 x 10^{14} cm^{-2}, i.e. ~5.5 x 10^{21} cm^{-3}. Moreover, the band structure and density of states of doped bilayer graphene **(Figure 5c,d)** show that the Fermi energy shifts upward from the Dirac point by ~0.54 eV compared to that of pristine bilayer graphene due to electron doping. Effective doping has previously been reported for graphene on metal substrates, [45-47] leading to a qualitatively comparable but lower energy shift in the Fermi energy (0.3 eV above the Dirac point).[46] The doping electrons in bilayer graphene exhibit high Fermi velocities because of the linear energy dispersion relation near the Dirac points. The carrier mobility (μ) in doped graphene can be calculated based on the doped electron density (n) and measured electrical conductivity (σ) according to the equation $\mu = \sigma/en$, where e is the electron charge, i.e. 1.602 x 10^{-19} C. The highest measured electrical conductivity of copper-embedded graphene during this investigation on a macroscale sample is ~1267 times higher than the conductivity of the surrounding matrix, i.e. ~7.1 x 10^{10} S m^{-1}. Therefore,

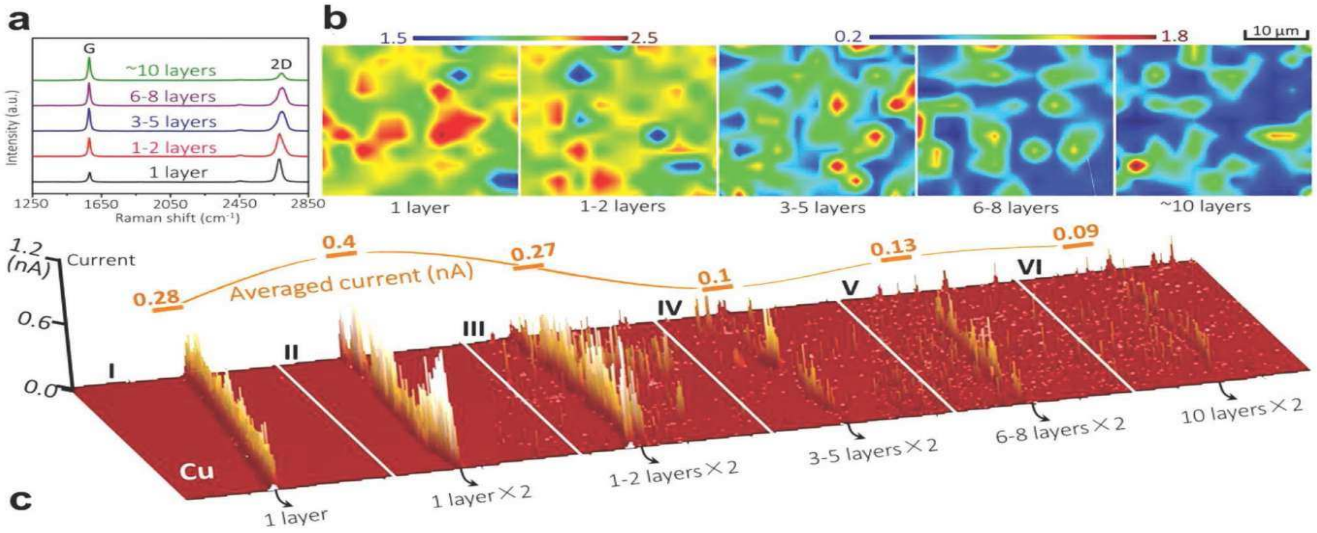

Figure 4. Influence of number of graphene layers on the electrical conductivity. a) Raman spectra of graphene deposited on copper foils by a CVD process with layer numbers ranging from one to ten. b) Mapping of the intensity ratio of the 2D peak to the G peak (I_{2D}/I_G) for the as-deposited graphene in a 30 μm x 30 μm area. A ratio of 2.1 indicates the monolayer nature of graphene.[44] c) A comparison of current flow in different Gr/Cu composites with varying graphene layer numbers. Composite I was fabricated by alternately stacking monolayer-Gr/Cu/monolayer-Gr foil and naked CVD foil, and the graphene was removed by reactive oxygen-ion etching. All other composites were fabricated according to the scheme depicted in Figure 1.

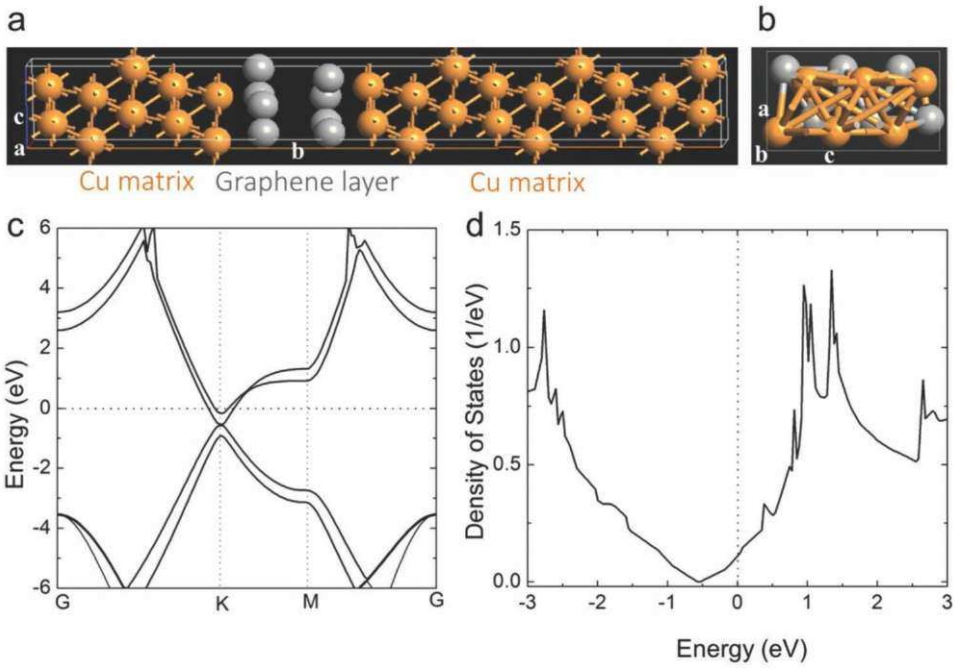

Figure 5. First-principles calculations. a,b) Model system for a Cu/bilayer-Gr/Cu composite. The bilayer graphene is stacked in an AB-model. The yellow and gray spheres denote Cu and C atoms, respectively. c) Electronic band structure. d) Density of states for doped graphene. The zero point denotes the Fermi energy.

the doped graphene is estimated to have an electron mobility of ~8 x 10^5 cm^2 V^{-1} s^{-1}, which is almost four times higher than the electron mobility measured in suspended graphene.[18] An increased electrical conductivity was also obtained for graphene embedded inside other metal matrices, such as Ag and Al (Figure S10, Supporting information), but not obtained when graphene was embedded inside semiconductor or polymer matrices, such as silicon and polymer polyethylene terephthalate (PET) (Figure S11, Supporting information).

As reported previously, a trade-off exists between electron mobility and electron density in suspended graphene or graphene interacting with elaborately designed substrates, [48-63] leading to not very high electrical conductivities in graphene (on the level of Cu or Ag). Here, we report a breakthrough in achieving a very high electron density while retaining high electron mobility in metal-embedded graphene. This leads to an about three orders of magnitude higher electrical conductivity. Therefore, the electron behavior in such graphene layers embedded in metals must be fundamentally different from that in suspended graphene, [13,22] graphene deposited on high-quality substrates, [23,24] or graphene covered with high-*k* dielectrics. [25,26]

3. Conclusion

In summary, we made a breakthrough on the trade-off between carrier mobility and carrier density in graphene, and realized high electron mobility and high electron density simultaneously in graphene by embedding it in metals through elaborate interface design and morphology control. As a result, an ultrahigh electrical conductivity, three orders of magnitude higher than the highest on record, is obtained in such embedded graphene. The hot-pressed graphene/metal configuration provides a novel platform to explore electron behavior in graphene, because it is fundamentally different from the previously reported systems such as suspended graphene, graphene deposited on high-quality substrates, and graphene covered with high-*k* dielectrics. In the corresponding graphene/Cu composites, an extremely low graphene volume fraction of only 0.008% is sufficient to yielding an electrical conductivity as high as ~117% IACS, which is significantly higher than that of Ag. Much higher electrical conductivities are expected in graphene/Cu composites with a sub-micro/nano-structure. The here presented results will open up new opportunities for graphene / copper applications, which could lead to higher efficiency and performance and less energy consumption in electrical and electronic applications.

4. Experimental Section

Fabrication of Gr/Cu Composite: Graphene was deposited on both sides of Cu foils via a chemical vapor deposition method. In a typical process Cu foils with a thickness of several tens of a micrometer were heated up to 1000 °C in a hydrogen/argon atmosphere and then methane was added for graphene growth. After finishing the deposition process, the Cu foils were cooled down to room temperature within 30 min. In order to prepare thicker (bulk) samples, several pieces of Gr-Cu-Gr foil were stacked on top of each other in a graphite mold and then hot-pressed (sintered) in an Ar atmosphere for 20 min at 900 °C in a linear press with a pressure of 50 MPa. Reference samples were also prepared under the same hot-pressing conditions. The typical thickness of a stacked and sintered sample was about 150 µm.

AFM Current Mapping on Interface: To evaluate the electrical properties along and across the interface areas, the electrical conductivity of a well defined area across the Cu/Gr/Cu interface was mapped using the contact current mode of an atomic force microscope with an applied voltage

of 2 V at room temperature. To ensure that each measurement was done with the same contact pressure and the same electrical contact conditions between the tip and the sample surface, the electric current test was carried out in the 'PeakForce TUNA' mode of a 'Bruker Dimension Icon and FastScan Bio' scanning probe AFM. For the measurement, one side of the Gr/Cu composite sample was attached and electrically connected to the sample holder using conductive silver paste, while a 2V measuring voltage was applied to a Pt coated Si-cantilever which was swept over the polished surface of the the other side of the sample. In this experiment, the applied peak force was 6 nN, the applied test voltage was 2 V and the current signals were peak currents measured at the cantilever.

First-Principles Calculation: First-principles calculation was carried out using the Vienna ab-initio simulation package (VASP) code.[64] The Cu/Gr bilayer/Cu composite was modeled by an AB-stacked bilayer graphene which was sandwiched between fourteen Cu(111) layers as shown in **Figure 3a**. The model system had a 3D periodicity. The lattice constant of the Cu is 3.614 Å. The interlayer distance of the AB-graphene is 3.430 Å, and the separation between the Cu and graphene is 2.210 Å, which is determined by minimization of the total energy. In our calculations, the projector augmented-wave method [65] was used for the wave function expansion with an energy cutoff at 500 eV. The local density approximation was adopted for the electron exchange and correlation. The Brillouin zone is sampled with 9 x 1 x 5 grid of the Monkhorst-Pack *k* points.[66] These calculation details were verified to provide accurate results. The total charge of the Cu/Gr bilayer/Cu system was obtained and the Bader charge was analyzed which is shown in Table S1 (Supporting Information). It shows that the graphene atoms have 32.480 valence electrons in total. The graphene obtained 0.480 electrons from the neighboring Cu atoms in total. This means that a primitive cell of the bilayer (containing four carbon atoms) is doped with 0.24 electrons. The band structure and the density of states **(Figure 4)** of the AB-bilayer graphene was also calculated using a primitive cell with 0.24 doping electrons by VASP. The lattice constant is 2.46 Å for the graphene. The Brillouin zone is sampled with 21 x 21 x 1 grid of the Monkhorst-Pack *k* points.

Supporting Information
Supporting Information is available from the Wiley Online Library or from the author.

Acknowledgements
This work was supported by the National Key R&D Program of China (No. 2017YFB0406200), the Natural Science Foundation of China (Nos. 51771110, 51371115, 51671130, 51771111, and 51131004), the Shanghai Science & Technology Committee (Nos. 15JC1402100 and 17520712400), the Ministry of Science & Technology of China (No. 2016YFE0130200), Hitachi Metals Ltd. and the International Copper Association. The authors thank Professors J. F. Jia and D. D. Guan for assistance in the scanning tunneling microscopy characterizations. Bruker Corporation in China is also acknowledged for allowing the use of the atomic force microscope and their assistance.

Conflict of Interest
The authors declare no conflict of interest.

Received: September 26, 2018,
Revised: January 12, 2019
Published online: August 14, 2019

Keywords
electrical conductivity, graphene, interface, metal matrix composites

[1] O. Hjortstam, P. Isberg, S. Söderholm, H. J. Dai, *Appl. Phys. A* **2004,** *78,* 1175.
[2] F. Yang, F. X. Wang, D. Zhang, J. Yang, D. Luo, Z. Xu, J. Wei, J.-Q. Wang, Z. Xu, F. Peng, X. Li, R. Li, Y. Li, M. Li, X. Bai, F. Ding, Y. Li, *Nature* **2014,** *510,* 522.
[3] K. S. Novoselov, A. K. Geim, S. V. Morozov, D. Jiang, Y. Zhang, S. V. Dubonos, I. V. Grigorieva, A. A. Firsov, *Science* **2004,** *306,* 666.
[4] C. Berger, Z. Song, T. Li, X. Li, A. Y. Ogbazghi, R. Feng, Z. Dai, A. N. Marchenkov, E. H. Conrad, P. N. First, W. A. de Heer,*J. Phys. Chem. B* **2004,** *108,* 19912.
[5] K. S. Novoselov, A. K. Geim, S. V. Morozov, D. Jiang, M. I. Katsnelson, I. V. Grigorieva, S. V. Dubonos, A. A. Firsov, *Nature* **2005,** *438,* 197.
[6] Y. B. Zhang, Y.-W. Tan, H. L. Stormer, P. Kim, *Nature* **2005,** *438,* 201.
[7] K. S. Novoselov, D. Jiang, F. Schedin, T. J. Booth, V. V. Khotkevich, S. V. Morozov, A. K. Geim, *Proc. Natl. Acad. Sci. USA* **2005,** *102,* 10451.
[8] C. Berger, Z. Song, X. Li, X. Wu, N. Brown, C. Naud, D. Mayou, T. Li, J. Hass, A. N. Marchenkov, E. H. Conrad, P. N. First, W. A. de Heer, *Science* **2006,** *312,* 1191.
[9] N. Stander, B. Huard, D. Goldhaber-Gordon, *Phys. Rev. Lett.* **2009,** *102,* 026807.
[10] K. I. Bolotin, F. Ghahari, M. D. Shulman, H. L. Stormer, P. Kim, *Nature* **2009,** *462,* 196.
[11] A. Tzalenchuk, S. Lara-Avila, A. Kalaboukhov, S. Paolillo, M. Syväjärvi, R. Yakimova, O. Kazakova, T. J. B. M. Janssen, V. Fal'ko, S. Kubatkin, *Nat. Nanotechnol.* **2010,** 5, 186.
[12] H. B. Heersche, P. Jarillo-Herrero, J. B. Oostinga, L. M. K. Vandersypen, A. F. Morpurgo, *Nature* **2007,** *446,* 56.
[13] X. Du, I. Skachko, A. Barker, E. Y. Andrei, *Nat. Nanotechnol.* **2008,** 3, 491.
[14] D. A. Bandurin, I. Torre, R. Krishna Kumar, M. Ben Shalom, A. Tomadin, A. Principi, G. H. Auton, E. Khestanova, K. S. Novoselov, I. V. Grigorieva, L. A. Ponomarenko, A. K. Geim, M. Polini, *Science* **2016,** *351,* 1055.
[15] L. Levitov, G. Falkovich, *Nat. Phys.* **2016,** *12,* 672.
[16] H. Guo, E. Ilseven, G. Falkovich, L. S. Levitov, *Proc. Natl. Acad. Sci. USA* **2017,** *114,* 3068.
[17] S. V. Morozov, K. S. Novoselov, M. I. Katsnelson, F. Schedin, D. C. Elias, J. A. Jaszczak, A. K. Geim, *Phys. Rev. Lett.* **2008,** *100,* 016602.
[18] K. I. Bolotin, K. J. Sikes, Z. Jiang, M. Klima, G. Fudenberg, J. Hone, P. Kim, H. L. Stormer, *Solid State Commun.* **2008,** *146,* 351.
[19] P. Neugebauer, M. Orlita, C. Faugeras, A.-L. Barra, M. Potemski, *Phys. Rev. Lett.* **2009,** *103,* 136403.
[20] W. Gannett, W. Regan, K. Watanabe, T. Taniguchi, M. F. Crommie, A. Zettl, *Appl. Phys. Lett.* **2011,** *98,* 242105.
[21] N. Petrone, C. R. Dean, I. Meric, A. M. van der Zande, P. Y. Huang, L. Wang, D. Muller, K. L. Shepard, J. Hone, *Nano Lett.* **2012,** *12,* 2751.
[22] A. S. Mayorov, D. C. Elias, I. S. Mukhin, S. V. Morozov, L. A. Ponomarenko, K. S. Novoselov, A. K. Geim, R. V. Gorbachev, *Nano Lett.* **2012,** *12,* 4629.
[23] X. Hong, A. Posadas, K. Zou, C. H. Ahn, J. Zhu, *Phys. Rev. Lett.* **2009,** *102,* 136808.
[24] C. R. Dean, A. F. Young, I. Meric, C. Lee, L. Wang, S. Sorgenfrei, K. Watanabe, T. Taniguchi, P. Kim, K. L. Shepard, J. Hone, *Nat. Nanotechnol.* **2010,** 5, 722.
[25] C. Jang, S. Adam, J.-H. Chen, E. D. Williams, S. D. Sarma, M. S. Fuhrer, *Phys. Rev. Lett.* **2008,** *101,* 146805.
[26] A. K. M. Newaz, Y. S. Puzyrev, B. Wang, S. T. Pantelides, K. I. Bolotin, *Nat. Commun.* **2012,** 3, 734.
[27] D.-B. Xiong, M. Cao, Q. Guo, Z. Q. Tan, G. L. Fan, Z. Q. Li, D. Zhang, *ACS Nano* **2015,** 9, 6934.
[28] J. Hwang, T. Yoon, S. H. Jin, J. Lee, T. Kim, S. H. Hong, S. Jeon, *Adv. Mater.* **2013,** 25, 6724.

[29] Y. K. Chen, X. Zhang, E. Z. Liu, C. N. He, C. S. Shi, J. J. Li, P. Nash, N. Q. Zhao, *Sci. Rep.* **2016,** 6, 19363.
[30] M. Cao, D.-B. Xiong, Z. Q. Tan, G. Ji, B. Amin-Ahmadi, Q. Guo, G. L. Fan, C. Q. Guo, Z. Q. Li, D. Zhang, *Carbon* **2017,** 7 77, 65.
[31] X. Li, W. Cai, J. An, S. Kim, J. Nah, D. Yang, R. Piner, A. Velamakanni, I. Jung, E. Tutuc, S. K. Banerjee, L. Colombo, R. S. Ruoff, *Science* **2009,** *324,* 1312.
[32] T. Yoon, W. C. Shin, T. Y. Kim, J. H. Mun, T.-S. Kim, B. J. Cho, *Nano Lett.* **2012,** 72, 1448.
[33] A. Nakamura, K. Matsunaga, J. Tohma, T. Yamamoto, Y. Ikuhara, *Nat. Mater.* **2003,** 2, 453.
[34] J. Seidel, L. W. Martin, Q. He, Q. Zhan, Y.-H. Chu, A. Rother, M. E. Hawkridge, P. Maksymovych, P. Yu, M. Gajek, N. Balke, S. V. Kalinin, S. Gemming, F. Wang, G. Catalan, J. F. Scott, N. A. Spaldin, J. Orenstein, R. Ramesh, *Nat. Mater.* **2009,** 8, 229.
[35] M. Fenn, G. Akuetey, P. E. Donovan,*J. Phys.: Condens. Matter* **1998,** *70,* 1707.
[36] K. Fuchs, *Math. Proc. Cambridge Philos. Soc.* **1938,** *34,* 100.
[37] E. H. Sondheimer, *Adv. Phys.* **1952,** 7, 1.
[38] A. F. Mayadas, M. Shatzkes, *Phys. Rev. B* **1970,** 7, 1382.
[39] J. M. Camacho, A. I. Oliva, *Thin Solid Films* **2006,** *575,* 1881.
[40] W. Li, D. Li, Q. Fu, C. Pan, *RSC Adv.* **2015,** 5, 80428.
[41] L. Gao, J. R. Guest, N. P. Guisinger, *Nano Lett.* **2010,** *70,* 3512.
[42] L. Zhao, K. T. Rim, H. Zhou, R. He, T. F. Heinz, A. Pinczuk, G. W. Flynn, A. N. Pasupathy, *Solid State Commun.* **2011,** *757,* 509.
[43] I. N. Kholmanov, C. W. Magnuson, A. E. Aliev, H. Li, B. Zhang, J. W. Suk, L. L. Zhang, E. Peng, S. H. Mousavi, A. B. Khanikaev, R. Piner, G. Shvets, R. S. Ruoff, *Nano Lett.* **2012,** *72,* 5679.
[44] A. C. Ferrari, J. C. Meyer, V. Scardaci, C. Casiraghi, M. Lazzeri, F. Mauri, S. Piscanec, D. Jiang, K. S. Novoselov, S. Roth, A. K. Geim, *Phys. Rev Lett.* **2006,** 97, 187401.
[45] A. Dahal, M. Batzill, *Nanoscale* **2014,** 6, 2548.
[46] A. L. Walters, S. Shu, A. Bostwick, K. S. Kim, L. Moreschini, Y. J. Chang, D. Innocenti, K. Horn, K. F. McCarty, E. Rotenberg, *Phys. Rev. B* **2011,** *84,* 195443.
[47] P. Sutter, J. T. Sadowski, E. Sutter, *Phys. Rev. B* **2009,** *80,* 245411.
[48] P. J. Zomer, S. P. Dash, N. Tombros, B. J. van Wees, *Appl. Phys. Lett.* **2011,** 99, 232104.
[49] J.-H. Chen, C. Jang, S. Adam, M. S. Fuhrer, E. D. Williams, M. Ishigami, *Nat. Phys.* **2008,** *4,* 377.
[50] M. Lafkioti, B. Krauss, T. Lohmann, U. Zschieschang, H. Klauk, K. v. Klitzing, J. H. Smet, *Nano Lett.* **2010,** *70,* 1149.
[51] J.-H. Chen, C. Jang, S. Xiao, M. Ishigami, M. S. Fuhrer, *Nat. Nanotechnol.* **2008,** 3, 206.
[52] N. Tombros, A. Veligura, J. Junesch, J. J. van den Berg, P. J. Zomer, M. Wojtaszek, I. J. Vera Marun, H. T. Jonkman, B. J. van Wees, *J. Appl. Phys.* **2011,** *709,* 093702.
[53] X. Hong, K. Zou, J. Zhu, *Phys. Rev. B* **2009,** *80,* 241415.
[54] E. H. Hwang, S. Das Sarma, *Phys. Rev. B* **2008,** 77, 115449.
[55] E. H. Hwang, S. Adam, S. Das Sarma, *Phys. Rev. Lett.* **2007,** 98, 186806.
[56] A. Guermoune, T. Chari, F. Popescu, S. S. Sabri, J. Guillemette, H. S. Skulason, T. Szkopek, M. Siaj, *Carbon* **2011,** *49,* 4204.
[57] T. Stauber, N. M. R. Peres, F. Guinea, *Phys. Rev. B* **2007,** *76,* 205423.
[58] Y.-W. Tan, Y. Zhang, K. Bolotin, Y. Zhao, S. Adam, E. H. Hwang, S. Das Sarma, H. L. Stormer, P. Kim, *Phys. Rev. Lett.* **2007,** 99, 246803.
[59] A. S. Mayorov, R. V. Gorbachev, S. V. Morozov, L. Britnell, R. Jalil, L. A. Ponomarenko, P. Blake, K. S. Novoselov, K. Watanabe, T. Taniguchi, A. K. Geim, *Nano Lett.* **2011,** 7 7, 2396.
[60] Z. H. Ni, L. A. Ponomarenko, R. R. Nair, R. Yang, S. Anissimova, I. V. Grigorieva, F. Schedin, P. Blake, Z. X. Shen, E. H. Hill, K. S. Novoselov, A. K. Geim, *Nano Lett.* **2010,** *70,* 3868.
[61] A. F. Young, P. Kim, *Nat. Phys.* **2009,** 5, 222.
[62] T. Ando, *J. Phys. Soc. Jpn.* **2006,** *75,* 074716.
[63] K. I. Bolotin, K. J. Sikes, J. Hone, H. L. Stormer, P. Kim, *Phys. Rev. Lett.* **2008,** *707,* 096802.
[64] G. Kresse, J. Furthmüller, *Phys. Rev. B* **1996,** *54,* 11169.
[65] P. E. Blöchl, *Phys. Rev. B* **1994,** *50,* 17953.
[66] H. J. Monkhorst, J. D. Pack, *Phys. Rev. B* **1976,** *73,* 5188.